2017

Dissipative elastic metamaterial with a lowfrequency passband

Yongquan Liu
Peking University

Jianlin Yi
Peking University

Zheng Li
Peking University, lizheng@pku.edu.cn

Xianyue Su
Peking University

Wenlong Li
University of Nebraska-Lincoln, wenlongli@unl.edu

See next page for additional authors

Authors

Yongquan Liu, Jianlin Yi, Zheng Li, Xianyue Su, Wenlong Li, and Mehrdad Negahban

Dissipative elastic metamaterial with a low-frequency passband

Yongquan Liu, Jianlin Yi, Zheng Li, Xianyue Su, Wenlong Li, and Mehrdad Negahban

View Online   Export Citation   CrossMark

ARTICLES YOU MAY BE INTERESTED IN

Acoustic metasurface-based perfect absorber with deep subwavelength thickness
Applied Physics Letters **108**, 063502 (2016); https://doi.org/10.1063/1.4941338

Elastic wave manipulation by using a phase-controlling meta-layer
Journal of Applied Physics **123**, 091708 (2018); https://doi.org/10.1063/1.4996018

Elastic metamaterial-based seismic shield for both Lamb and surface waves
AIP Advances **7**, 075015 (2017); https://doi.org/10.1063/1.4996716

Dissipative elastic metamaterial with a low-frequency passband

Yongquan Liu,[1] Jianlin Yi,[1] Zheng Li,[1,a] Xianyue Su,[1] Wenlong Li,[2] and Mehrdad Negahban[2]

[1]*Department of Mechanics & Engineering Science, LTCS, Peking University, Beijing 100871, China*
[2]*Mechanical & Materials Engineering, University of Nebraska-Lincoln, Lincoln, Nebraska 68588-0526, USA*

We design and experimentally demonstrate a dissipative elastic metamaterial structure that functions as a bandpass filter with a low-frequency passband. The mechanism of dissipation in this structure is well described by a mass-spring-damper model that reveals that the imaginary part of the wavenumber is non-zero, even in the passband of dissipative metamaterials. This indicates that transmittance in this range can be low. A prototype for this viscoelastic metamaterial model is fabricated by 3D printing techniques using soft and hard acrylics as constituent materials. The transmittance of the printed metamaterial is measured and shows good agreement with theoretical predictions, demonstrating its potential in the design of compact waveguides, filters and other advanced devices for controlling mechanical waves. © 2017 Author(s). *All article content, except where otherwise noted, is licensed under a Creative Commons Attribution (CC BY) license (http://creativecommons.org/licenses/by/4.0/).* [http://dx.doi.org/10.1063/1.4991034]

Propagation of waves in heterogeneous or inhomogeneous media is of great importance in scientific and technological research. In the past decades, artificially designed sub-wavelength materials with exceptional effective properties, termed as metamaterials,[1–3] have generated an ever-changing research field dedicated to manipulating waves in previously unimaginable ways. In elastodynamics, the first elastic metamaterial with negative effective density was proposed by Liu *et al*[4] based on the idea of local resonance. Subsequently, elastic metamaterials with negative Young's modulus,[5] double negativity,[6–9] fluid-like behavior[10,11] and other special characteristics have been developed. Many unusual functionalities, such as vibration attenuation,[4,5,12,13] negative refraction,[8,9,14] super-lensing[15] and invisibility to elastic waves,[16,17] have been proposed. It is worth mentioning that in general the elastic metamaterials possess negative effective parameters only in certain narrow frequency regions, corresponding to band-gap. Narisetti *et al*[18] showed that a monoatomic chain with ground-springs may act like a pass-band filter. Very recently, we[19] theoretically proposed an elastic metamaterial with negative effective parameters almost at all frequencies other than for a certain region, which corresponds to the band-pass range. Regarding the potential in the design of small-size waveguides, filters and other devices, the experimental realization of such elastic metamaterials is described in the present work.

It is well known that elastic metamaterials are designed based on the localized resonant mechanism in the material. Silicon rubber, foam and other polymers are usually combined to achieve low-frequency resonance[4,9,12] or to make tunable metamaterials.[20] Although polymers are typically viscoelastic materials and have dynamic moduli that are complex and frequency-dependent, for simplicity they are usually treated as linear elastic materials. The difference between using elastic and viscoelastic properties may lead to significant alterations in the effective parameters or dispersion

---

[a]Author to whom correspondence should be addressed. Electronic mail: lizheng@pku.edu.cn

characteristics. For example, researchers have theoretically shown that viscoelasticity would widen band gaps, shift band gaps to lower frequencies or both.[21–24] In the passband, the transmission is generally worsened for locally resonant metamaterials.[25] In addition, the damping phenomena of dissipative metamaterials may exhibit high dissipation throughout the spectrum,[26] which can be used for broadband blast wave mitigation.[27,28] In comparison to the extent of theoretical research, very few experimental studies have been reported to date on such metamaterials.

We present a theoretical study and experimental realization of a dissipative elastic metamaterial with a low-frequency passband. The metamaterial is described by a mass-spring-damper model. By using the Kelvin-Voigt mechanical analog, the effects of using viscoelastic materials is investigated. This shows that the dissipation of our bandpass-type viscoelastic metamaterial will lead to a narrower passband. This elastic metamaterial is fabricated and tested to show agreement with theoretical predictions.

Fig. 1(a) presents a unit cell of the proposed elastic metamaterial that shows a low-frequency passband. A hard acrylic cylinder, with radius 3.5 mm and height 8 mm, was encased in a soft acrylic material to shape a cylinder with radius 5 mm and height 10 mm. The soft-covered hard acrylic cylinder was then itself encased in a hard acrylic cylindrical shell, whose outer radius and height are 7.5 mm and 10 mm, respectively. The outer boundary of the hard acrylic shell was fixed. In the axial direction, this system was repeated so as to construct unit cells that are arranged periodically to form the elastic metamaterial. The hard acrylic has a Young's modulus $E_a = 2.19$ GPa, Poisson's ratio $v_a = 0.39$ and density $\rho_a = 1187$ kg/m^3; whereas the soft acrylic has a Young's modulus $E_f = 0.78$ MPa, Poisson's ratio $v_f = 0.34$ and density $\rho_f = 1124$ kg/m^3. The passband structure (of longitudinal waves)
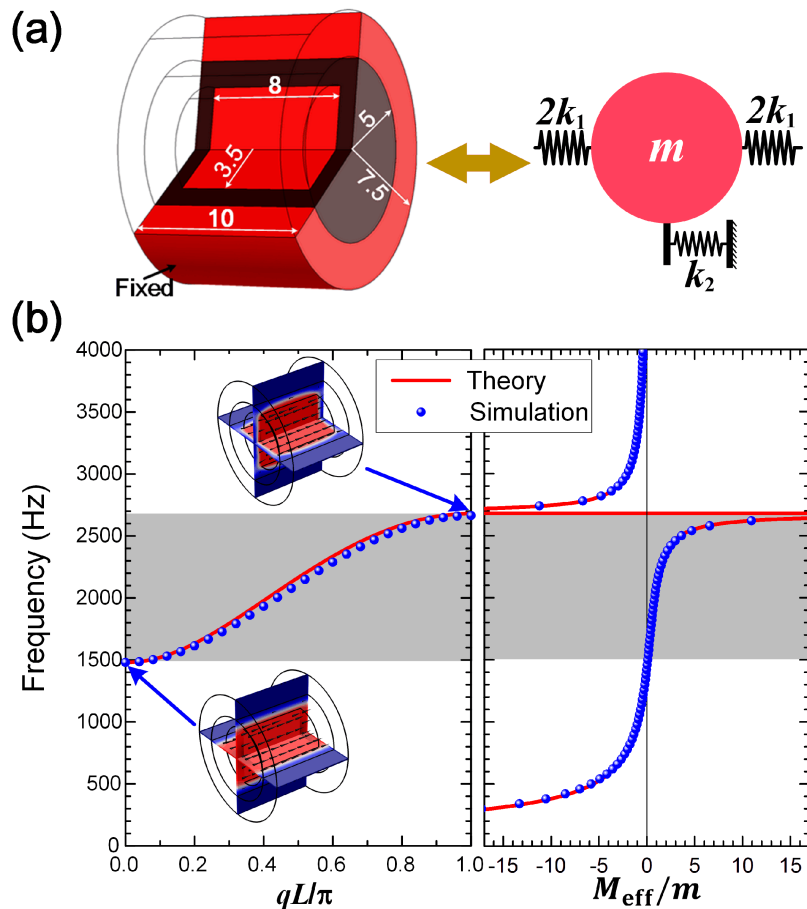

FIG. 1. (a) Unit cell of the elastic metamaterial with a low-frequency passband and its mass-spring model; (b) the band structure and dimensionless effective mass of a non-dissipative system. The grey region corresponds to the passband. The mode shapes at starting and ending frequencies of the passband are shown in the inset.

and dimensionless effective mass of this metamaterial were calculated numerically using COMSOL MULTIPHYSICS, as shown in Fig. 1(b). Due to the fixed boundary of the outer shell, the proposed elastic metamaterial always shows negative effective mass except for a fixed range of (1480, 2680) Hz. The negative mass will lead to an imaginary wave number, indicating that the wave will decay exponentially. Therefore, the propagating mode of this system only lies in a low-frequency range. The mode shapes at starting and ending frequencies of the passband are plotted as insets in Fig. 1(b), indicating that the passband is caused by the resonance of the hard acrylic resonator. Other branches of propagating waves, such as torsional and flexural modes, possess similar passband characters.

In the passband region, the longitudinal wavelength for the hard acrylic material is from 716 to 1296 mm, which is around two orders of magnitude larger than the size of the unit cell. This feature allows us to treat the resonator and the outer shell as rigid bodies. As a result, the fixed outer boundary can be easily achieved just by fixing a small part of the hard outer shell. In addition, the rigid outer shell provides the metamaterial sufficient rigidity for practical applications. To illustrate its mechanisms clearly, the proposed elastic metamaterial was analyzed as an elastic system using a mass-spring model, as illustrated in the right part of Fig. 1(a). It should be noted that this model has been used by Yao *et al*[29] to investigate structures with negative effective mass below a cut-off frequency. In this model, the mass is $m = \rho_a V_a + \rho_f V_f$, where V_a and V_f are volumes of the hard acrylic resonator and the soft acrylic coat, respectively. The stiffness of the springs can be calculated as

$$k_1 = \frac{m}{4}\left(\omega_2^2 - \omega_1^2\right), \quad k_2 = m\omega_1^2 \tag{1}$$

where $\omega_1 = 1480$ Hz and $\omega_2 = 2680$ Hz are the starting and ending frequencies of the passband, respectively. Details of the mass-spring model are provided in the supplementary material. For comparison, the band structure and effective mass based on the mass-spring model are also plotted as solid red lines (termed as "theory") in Fig. 1(b), which matches the numerical results perfectly.

To better describe the behavior of elastic metamaterials, the damping or dissipation of the component materials, especially for the soft acrylic material, should be considered. We study the dissipation of metamaterials by changing the linear elastic springs of stiffness k_i in the elastic mass-spring model by Kelvin-Voigt spring-damper analogs. These are represented by a purely viscous dashpot c_i and a purely elastic spring k_i connected in parallel as shown in Fig. 2(a). By introducing the dimensionless damping coefficients $\tau_i = c_i/\sqrt{mk_i}$, we can obtain the dispersion
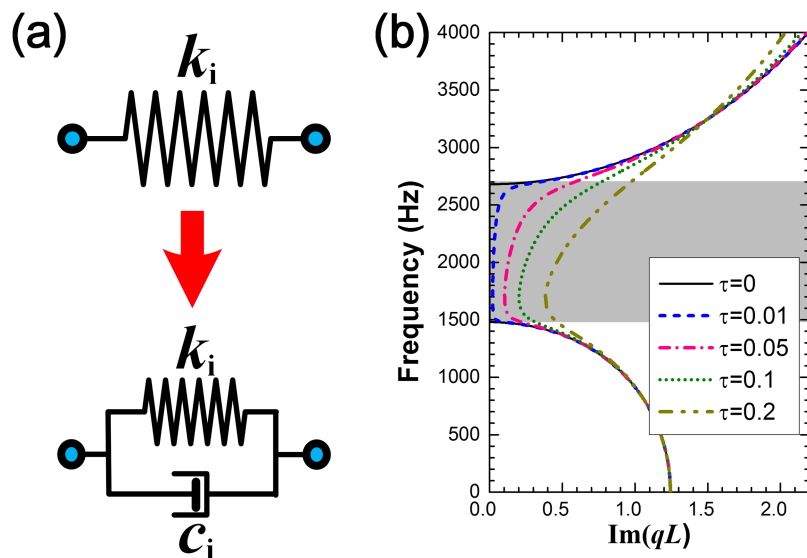

FIG. 2. (a) The effect of dissipation is investigated by changing each linear elastic spring by a Kelvin-Voigt viscoelastic solid analog; (b) imaginary part of the dimensionless wavenumber of the dissipative metamaterial. The grey region corresponds to the passband of the non-dissipative case.

equations theoretically in the dissipative case. Fig. 2(b) shows the imaginary part of the dimensionless wavenumber Im (qL) for metamaterials with different damping coefficients $\tau = \tau_1 = \tau_2$, representing the attenuation of mechanical waves. For comparison, the passband of the non-dissipative case are highlighted by coloring it as a grey region. Naturally, Im $(qL) = 0$ in the passband of non-dissipative metamaterials ($\tau = 0$). However, even in the passband, this is always non-zero for dissipative metamaterials. The value of Im (qL) increases with the damping coefficients τ, indicating that mechanical waves cannot propagate in highly dissipative metamaterials with large unit cells.

Considering that elastic metamaterials with finite unit cells are usually applied in practice, the effects of the dissipation can be further investigated by evaluating transmission properties of finite elastic metamaterials. Fig. 3(a) shows a finite elastic metamaterial with N periods. If a displacement u_{in} is applied on the left side of the finite metamaterial, the transmittance defined as $|t| = u_{out}/u_{in}$ can be derived theoretically, where u_{out} is the output displacement of the structure on the right side. The transmittance of a five-period elastic metamaterial with different damping coefficients τ are illustrated in Fig. 3(b). For the cases of non-dissipative ($\tau = 0$) or quasi non-dissipative ($\tau = 0.01$) materials, the passband are very close to those obtained from the dispersion curve (the grey region). It is worth noting that five peaks appear in the passband due to the resonance of the finite metamaterial. In fact, the number of small peaks will increase with the periods N.[19] Nevertheless, with the rise of the damping coefficients τ, these small peaks gradually disappear with lower transmittance. From a practical point of view, one can define the passband of finite dissipative metamaterials as long as the transmittance is greater than a certain value, such as 0.3. Intuitively, the passband gets narrower for the case of higher damping coefficients. For example, it is respectively (1437, 2414) Hz and (1461, 2146) Hz for the cases of $\tau = 0.05$ and $\tau = 0.1$. Moreover, there is no passband if the damping coefficient becomes 0.2. Apart from this, the passband also becomes narrower with the increase of
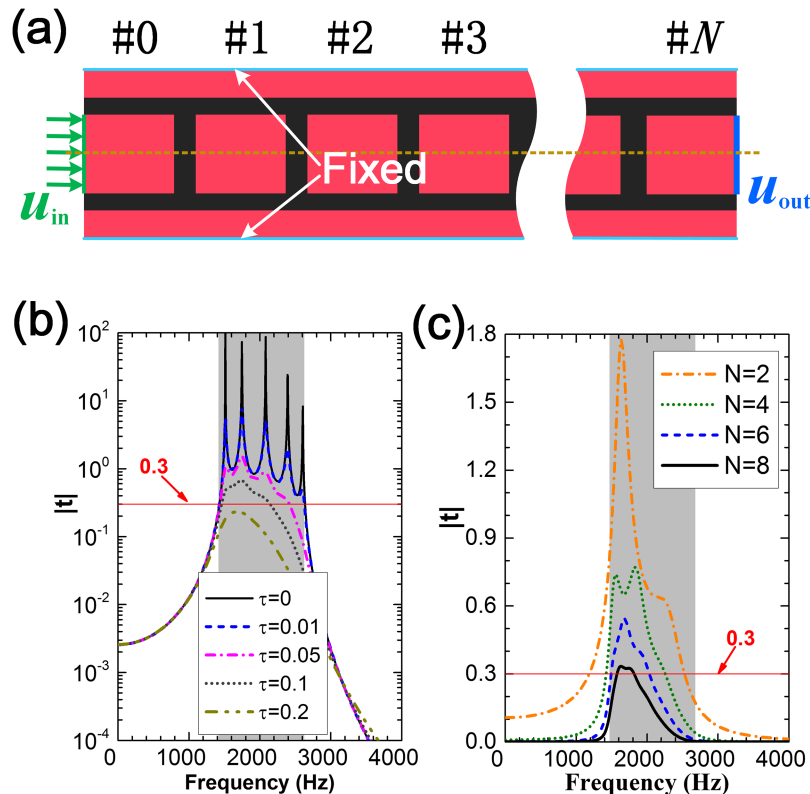

FIG. 3. (a) Schematic of a finite elastic metamaterial with N periods; (b) transmittance of a 5-period elastic metamaterial with different damping coefficients; (c) transmittance of elastic metamaterials with different number periodic units, the damping coefficient is set as $\tau = 0.1$. The grey regions in (b) and (c) correspond to the passband of the non-dissipative elastic case.

period *N*, as shown in Fig. 3(c). When a damping coefficient τ = 0.1 is set, the passband changes from (1185, 2527) Hz for *N*=2 to (1578, 1818) Hz for *N*=8.

To demonstrate the feasibility of using an elastic-based design and the effects of dissipation on our proposed elastic metamaterial, we built a prototype and perform an experimental investigation. A five-period elastic metamaterial was fabricated using a material-selectable three-dimensional (3D) printing system (Stratasys, Objet 500 Connex3). The printed system was clamped using a vise to achieve the fixed boundary condition, as illustrated in Fig. 4(a). A shaker (Mini-Shaker, Type 4810) was super-glued to the acrylic resonator at one end of the sample. At the other end of the sample, a laser Doppler vibrometer (Polytec, PSV-400) was aligned to the resonator part for the measurement of its response at different frequencies. Details of the sample fabrication and testing are provided in the supplementary material. Fig. 4(b) shows the measured frequency response of this five-period elastic metamaterial (red dots). For comparison, the theoretical transmittance is plotted as the red solid line based on the model of dissipative metamaterials described above, where the damping coefficient τ = 0.1 is used. If recognized as $|t| \geq 0.3$, the passband of this finite dissipative metamaterial is measured as about (1440, 2240) Hz, which is in agreement with the theoretical predictions of (1461, 2146) Hz.

We then tested the transmittance of a seven-period elastic metamaterial to verify the bandpass feature of our dissipative metamaterial further, which is plotted as the blue triangles in Fig. 4(b), showing that the passband range measured experimentally is reduced to about (1500, 1750) Hz, compared with the theoretical results of (1535, 1925) Hz with the same damping coefficient τ = 0.1. Therefore, the dissipation of our passband-type metamaterial is a feature that cannot be ignored. This result also provides justification for setting the damping coefficient as τ = 0.1. The deviation of the theoretical model and the tested results is observed due to the simplified model. Better agreement
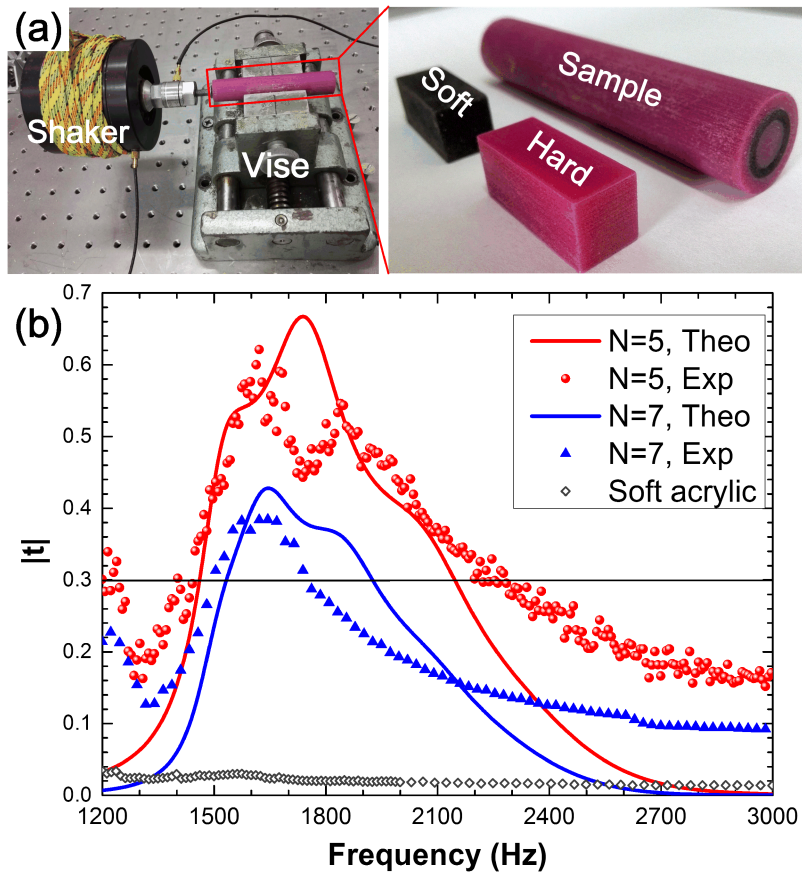

FIG. 4. (a) Photographic images of the vibration exciter and the specimen; (b) experimental and theoretical transmittances for different samples.

are expected if the frequency dependence of the damping coefficient is considered. Moreover, we fabricated a sample without resonators to use for comparative studies. The dimensions of this sample are the same as the five-period system, but the inner resonators are replaced by the soft acrylic material. This sample can be regarded as a typical elastic metamaterial with a bandgap over the entire low-frequency region.[29] The measured frequency response is plotted in Fig. 4(b) as the black hollow rhombuses. It indicates that there is no passband in this case, which can also be explained theoretically and numerically.

In conclusion, we have theoretically investigated and experimentally demonstrated a dissipative elastic metamaterial with a low-frequency passband. Our metamaterial could be interpreted by using the Kelvin-Voigt model, revealing that the dissipation of our band-pass-type elastic metamaterial could not be ignored. The passband becomes narrower with the increase of the damping coefficients and also with increasing the length of the metamaterial. The elastic metamaterial was 3D printed using a soft and a hard acrylic as the two constituent materials, and was experimentally evaluated to show agreement with theoretical predictions. The present study provides intriguing possibilities to design compact waveguides, filters and other advanced devices for elastic waves.

SUPPLEMENTARY MATERIAL

See supplementary material for detailed analyses on the mass-spring model, transmittance of finite elastic metamaterials, process of sample fabrication & testing, and the numerical results of foam surrounded by fixed acrylic shell.

ACKNOWLEDGEMENTS

[1] D. R. Smith, W. J. Padilla, D. C. Vier, S. C. Nemat-Nasser, and S. Schultz, Phys. Rev. Lett. **84**, 4184 (2000).
[2] R. A. Shelby, D. R. Smith, and S. Schultz, Science **292**, 77–79 (2001).
[3] D. R. Smith, J. B. Pendry, and M. C. Wiltshire, Science **305**, 788–792 (2004).
[4] Z. Liu, X. Zhang, Y. Mao, Y. Y. Zhu, Z. Yang, C. T. Chan, and P. Sheng, Science **289**, 1734–1736 (2000).
[5] H. H. Huang and C. T. Sun, J. Mech. Phys. Solids **59**, 2070–2081 (2011).
[6] J. Li and C. T. Chan, Phys. Rev. E **70**, 055602 (2004).
[7] Y. Ding, Z. Liu, C. Qiu, and J. Shi, Phys. Rev. Lett. **99**, 093904 (2007).
[8] X. N. Liu, G. K. Hu, G. L. Huang, and C. T. Sun, Appl. Phys. Lett. **98**, 251907 (2011).
[9] Y. Wu, Y. Lai, and Z. Q. Zhang, Phys. Rev. Lett. **107**, 105506 (2011).
[10] Y. Lai, Y. Wu, P. Sheng, and Z. Q. Zhang, Nature Mater. **10**, 620–624 (2011).
[11] G. Ma, C. Fu, G. Wang, P. Del Hougne, J. Christensen, Y. Lai, and P. Sheng, Nature Commun. **7**, 13536 (2016).
[12] Y. Liu, X. Su, and C. T. Sun, J. Mech. Phys. Solids **74**, 158–174 (2015).
[13] T. L. Smith, K. Rao, and I. Dyer, Noise Control Eng. J. **26**, 56–61 (1986).
[14] R. Zhu, X. N. Liu, G. K. Hu, C. T. Sun, and G. L. Huang, Nature Commun. **5**, 5510 (2014).
[15] J. H. Oh, H. M. Seung, and Y. Y. Kim, Appl. Phys. Lett. **104**, 073503 (2014).
[16] M. Farhat, S. Guenneau, and S. Enoch, Phys. Rev. Lett. **103**, 024301 (2009).
[17] N. Stenger, M. Wilhelm, and M. Wegener, Phys. Rev. Lett. **108**, 014301 (2012).
[18] R. K. Narisetti, M. J. Leamy, and M. Ruzzene, J. Vib. Acoust. **132**, 031001 (2010).
[19] Y. Liu, X. Shen, X. Su, and C. T. Sun, J. Vib. Acoust. **138**, 021011 (2016).
[20] P. Wang, F. Casadei, S. Shan, J. C. Weaver, and K. Bertoldi, Phys. Rev. Lett. **113**, 014301 (2014).
[21] I. E. Psarobas, Phys. Rev. B **64**, 012303 (2001).
[22] Y. P. Zhao and P. J. Wei, Comput. Mater. Sci. **46**, 603–606 (2009).
[23] M. I. Hussein and M. J. Frazier, J. Appl. Phys. **108**, 093506 (2010).
[24] J. M. Manimala and C. T. Sun, J. Appl. Phys. **115**, 023518 (2014).
[25] Y. F. Wang, Y. S. Wang, and V. Laude, Phys. Rev. B **92**, 104110 (2015).
[26] M. I. Hussein and M. J. Frazier, J. Sound Vib. **332**, 4767–4774 (2013).
[27] Y. Y. Chen, M. V. Barnhart, J. K. Chen, G. K. Hu, C. T. Sun, and G. L. Huang, Compos. Struct. **136**, 358–371 (2016).
[28] H. Chen, X. P. Li, Y. Y. Chen, and G. L. Huang, Ultrasonics **76**, 99–108 (2016).
[29] S. Yao, X. Zhou, and G. Hu, New J. Phys. **12**, 103025 (2010).